Spectroscopy, dynamics, and chaos of the CS_2 molecule: Fourier transform and phase-space analysis

J. P. Pique[a] and M. Joyeux
Laboratoire de Spectrométrie Physique, Université Joseph Fourier de Grenoble,[b] Boite Postale 87, 38402 Saint-Martin-d'Hères Cedex, France

J. Manners
The Open University, Physics Department, Walton Hall, Milton Keynes, MK7 6AA, United Kingdom

G. Sitja
Laboratoire de Spectrométrie Physique, Universite Joseph Fourier de Grenoble,[b] Boite Postale 87, 38402 Saint-Martin-d'Hères Cedex, France

(Received 1 May 1991; accepted 27 August 1991)

In this paper we analyze the vibrational spectra of the Σ_g^+ ground state of CS_2, the experimental results of which have been described in a forth coming paper. We show that, up to 12 000 cm^{-1}, CS_2 can be described by a system of two degrees of freedom strongly coupled by a 1:2 type Fermi resonance. The corresponding vibrational spectra are refitted with the aid of only seven parameters. Analysis of the spectra by the statistical Fourier transform technique reveals stroboscopic effects between the symmetric stretching mode and the bending mode. The distinction between the "stroboscopic hole" due to these effects and the "correlation hole" due to nonintegrable terms in the Hamiltonian is discussed in detail. The study of the topology of the phase space of CS_2 in the regular and chaotic cases is carried out in the basis described by a vibrational angular momentum which includes the Fermi resonance. We show the analogy between the localization of the wave packets of the eigenstates and the trajectories. We also show the destabilization of the trajectories due to a term in the Hamiltonian which couples neighboring polyads and which is a second Fermi resonance. We show that only two resonances are enough to induce a chaotic situation.

I. INTRODUCTION

The manifestation of classically chaotic phenomena in quantum systems ("quantum chaos") has been studied in detail theoretically to the semiclassical limit.[1] For real systems such as molecules, the challenge is to understand the consequences of such situations especially during chemical reactions. In molecules, chaos generally appears at very high vibrational energies. It is important to know if spectroscopy can shed any light on the problem. The difficulty of accessing high energies explains the relative small number of experimental data in existence up to the present. Some experiments have already provided some partial answers. In the stimulated emission pumping (SEP) spectra of the ground state of the C_2H_2 molecule at an energy of 28 000 cm^{-1}, Abramson *et al.*[2] have, for the first time, discovered a situation comparable to that observed in nuclear physics.[3] The molecular dynamics of C_2H_2 has subsequently been studied in detail over a wide energy range by the statistical Fourier transform[4] (SFT) technique which reveals vibrational energy redistribution on several time scales and a new mode which may be a promoter of chemical reactions.[5] Haller, Koppel, and Cederbaum[6] are the first to have analyzed the statistical properties of the NO_2 molecule around 15 000 cm^{-1} and have found a repulsion between levels which implies chaos. An extensive experimental study has recently been carried out by Jost *et al.*[7] Levandier *et al.*[8] have shown that, for the methylglyoxal molecule, the Fourier transform of the intense magnetic field level anticrossing spectrum contains a hole which is still unexplained because its width is a twentieth of the time corresponding to the density of states. Broyer *et al.*[9] have shown that the chaotic character of the Na_3 molecule seems to be linked with a very soft mode of its linear configuration. In contrast, Bentley *et al.*[10] have shown that the HCN molecule is not chaotic at the energies predicted by theory. This disagreement is probably due to the fact that quantum mechanics integrates irregularities in the potential which are smaller than the wavelength, whereas classical mechanics is very sensitive to irregularities which can easily destabilize the classical trajectories. Lastly, Yamanouchi *et al.*[11] have shown that the SO_2 molecule remains very regular and even very harmonic until at least 18 000 cm^{-1}.

In general, the loss of good vibrational quantum numbers in molecules which are excited in regions where they show chaotic motion, and the breaking of the selection rules which follows from this, make the spectra complex and unassignable. Using methods based on the study of spectral correlations and, in particular, the SFT technique,[8,12] it is possible (at least in the region of maximum chaos) to extract information about the molecular dynamics, as long as the density of states is large enough so that the total number of states in the energy interval under investigation is statistically significant (several hundred levels). However, small

[a] To whom correspondence should be addressed.
[b] Associated to CNRS (LA08).

molecules of three atoms are theoretically tractable. The relative simplicity of their spectra and, thus, of their Fourier transform, render possible, both the study of the transition to chaos and the modelling of the molecule. The understanding of the physic origin of chaos will be of great interest. The Fourier transform, which is a powerful toll in the semi-classical limit,[13-15] becomes calculable.

We believe that the experimental and theoretical study of a triatomic molecule like CS_2 can be useful to study pure vibrational chaos. A molecule with heavy atoms has the advantage of having vibrational modes that are relatively soft ($\nu_1 = 673$ cm^{-1}, $\nu_2 = 398$ cm^{-1}, $\nu_3 = 1559$ cm^{-1}) and, therefore, provides a large density of states at a given energy. Furthermore, CS_2 is subject to very strong anharmonicities and Fermi resonances, which are necessary conditions for the rapid establishment of chaos. We will see that, because the antisymmetric stretching mode does not easily couple to other modes, it is possible to study the dynamics of CS_2 in a subspace of two degrees of freedom up to relatively high energies. In contrast with the theoretical work of Kato,[16] this subspace is not the symmetric and antisymmetric stretching space but a space where the bending and symmetric stretching modes, which belong to the same vibrational symmetry, are strongly coupled. Finally, because the ground electronic state Σ_g^+ of CS_2 is well isolated, it is possible to carry out a study of pure vibrational chaos. In the linear ground electronic state, there is no overlap with and no perturbation due to other electronic states up to 26 187 cm^{-1} where the first excited state appears (referred to as the R state by Kleman[17]). It would seem, then, that CS_2 is a good candidate for a study of the transition towards vibrational chaos.

In Ref. 18 we present resolved fluorescence spectra for the Σ_g^+ state of CS_2 up to 18 000 cm^{-1} and discussed the fit of the levels up to 12 000 cm^{-1} with the aid of an integrable Hamiltonian. In this paper we will first discuss the reduction of the vibrational Hamiltonian of CS_2 to a system of two degrees of freedom. Then we will describe the effect of anharmonicities and integrable and nonintegrable Fermi resonances couplings using Fourier transform analysis. Finally, by using a theory developed by Kellman,[19] we will construct a semiclassical Hamiltonian for CS_2 from the experimental results and analyze the topology of the phase space. We will establish the clear link that exists between the classical and the quantum object.

II. THE EFFECTIVE HAMILTONIAN FOR CS_2 IN TWO DIMENSIONS

In Ref. 18 we presented the fit of the dispersed fluorescence spectrum of CS_2 with the aid of a Hamiltonian which describes the vibrational spectrum of the Σ_g^+ ground state of CS_2 up to 12 000 cm^{-1}. In the normal basis, the absence of coupling between the antisymmetric stretching mode and the other two modes makes the Hamiltonian block diagonal. The block which corresponds to $v_3 = 0$ describes the strong 1:2 Fermi resonance between the symmetric stretching mode and the bending mode. In this block, the couplings between adjacent polyads can be easily introduced. 70% of the levels observed experimentally on excitation in the 15 V band and 100% of those observed by excitation in the 10 V band belong to this block. This group of levels corresponds to $l'' = 0$ and even v_2''. In this paper we will study the dynamics of CS_2 in a two-dimensional subspace.

We have once again fitted the levels corresponding to this subspace with the aid of a two-dimensional Hamiltonian. It describes two coupled anharmonic oscillators. The diagonal part is written as

$$H_0 = \omega_1'(v_1 + \tfrac{1}{2}) + \omega_2'(v_2 + 1) + X_{11}(v_1 + \tfrac{1}{2})^2 + X_{22}(v_2 + 1)^2 + X_{12}(v_1 + \tfrac{1}{2})(v_2 + 1) + Y_{222}(v_2 + 1)^3. \quad (1)$$

The lowest-order Fermi term which mixes states of the same polyad (the number of which is defined by $N = v_1 + v_2/2$) is

$$H_F = -(1/\sqrt{2})k_{122}v_1^{1/2}(v_2 + 2). \quad (2)$$

The higher-order 1:2 resonance terms described by the parameters λ_1 and λ_2 do not significantly improve the fit to our experimental data. Table I shows the result obtained using only seven parameters. This reduction to two dimensions modifies the values of ω_1 and ω_2 in ω_1' and ω_2' since the vibrational quantum defects arising from the terms in $v_3 + \frac{1}{2}$ are carried over into the harmonic parameters,

$$\omega_1' = \omega_1 + \tfrac{1}{2}X_{13},$$
$$\omega_2' = \omega_2 + \tfrac{1}{2}X_{23}. \quad (3)$$

It is important to note that at very high vibrational energies, the antisymmetric stretching mode ν_3 will become coupled to the others and the simplification that we have just made will no longer be valid. Taking account of the strong coupling between the ν_1 and ν_2 modes which occurs from very low energies, we believe that, in CS_2, the transition to chaos will appear initially in a two-dimensional subspace rather than arising from couplings which mix equally all three modes of the molecule (as in a random matrix).

We also consider a term which couples adjacent polyads for which $\Delta N = \pm 1$ ($N = \nu_1 + \nu_2/2$) is given by

TABLE I. Vibrational parameters of the two-dimensional Hamiltonian of CS_2 (see text). λ_i fixed to Bernath's values (see Ref. 18) or fixed to zero.

Parameters	λ_i fixed	$\lambda_i = 0$
ω_1'	668.60 ± 0.69	661.83 ± 0.77
ω_2'	395.13 ± 0.34	396.79 ± 0.46
x_{11}	-1.001 ± 0.024	-0.181 ± 0.042
x_{22}	1.190 ± 0.044	0.719 ± 0.116
x_{12}	-3.103 ± 0.028	-1.206 ± 0.377
y_{222}	-0.006 ± 0.001	-0.0112 ± 0.0011
k_{122}	41.71 ± 1.62	41.114 ± 4.38
λ_1	0.491	0
λ_2	0.459	0
eqm (cm^{-1})	0.26	0.33

$$H_c = -\tfrac{1}{2}k_{1122}v_1^{1/2}(v_1-1)^{1/2}(v_2+2)$$
$$(\Delta v_1 = \pm 2,\ \Delta v_2 = \pm 2). \tag{4}$$

As we will see later, couplings of this type may be responsible for the onset of chaos in CS_2 and could be responsible for accidental perturbations observed[18] in the fluorescence spectrum of CS_2 below 12 000 cm^{-1}. H_c is just an example among several terms which couple adjacent polyades, but, for the purpose of this paper, it is not necessary to consider all of them since they give the same kind of results that we will discuss now.

The order of magnitude of the coupling parameters in CS_2 (see Table I) shows clearly that, from low energies ($E < 5000$ cm^{-1}), the normal basis set is far from being a good one. A crucial problem for the study of vibrational chaos in molecules is to define the best basis for the integrable part of the Hamiltonian. Since, in molecules, resonances are the rule rather than the exception, it is clear that this basis must include the relevant integrable resonances. Before tackling this problem in detail in Sec. IV, we are going to show, taking the example of CS_2, how the anharmonicities, the Fermi resonances, and the nonintegrable couplings manifest themselves in the Fourier transform of the molecular spectra.

III. FOURIER TRANSFORM SPECTRUM OF THE Σ_g^+ STATE OF CS_2

The Fourier transform (FT) of a spectrum is not only a mathematical operation which transforms the energy domain into the time domain but, in fact, the square of the FT reveals information which is obscured in the complicated direct spectrum: it shows up interferences between energy levels which are weighted by Franck–Condon factors.[8,12] In the next paragraph we will show, by the analysis of $|FT|^2$, the effects of spectral regularities, anharmonicities, and spectral correlations on the complete set of levels generated by the Hamiltonian of CS_2 fitted earlier.

It is always theoretically possible under these conditions to use a Dirac spectrum,

$$I(E) = \sum_{n,m} \delta(E - E_{n,m}), \tag{5}$$

where

$$n = v_1 + \tfrac{1}{2} \quad \text{(symmetric stretching)},$$
$$m = v_2 + 1 \quad \text{(bending)}. \tag{6}$$

If we limit ourselves initially to the diagonal part of the Hamiltonian we have

$$E_{nm} = \omega_1' n + \omega_2' m + X_{11}n^2 + X_{22}m^2 + X_{12}nm + Y_{222}m^3. \tag{7}$$

The FT of the spectrum is given by

$$C(t) = \sum_{nm} e^{2i\pi \frac{E_{nm}t}{h}}. \tag{8}$$

The modulus squared of the FT which may also be viewed as the survival probability of the wave packet [described by Eq. (5)], is

$$|C(t)|^2 = 2\sum_{\Delta E>0} \cos 2\pi \frac{\Delta E t}{h}, \tag{9}$$

where

$$\Delta E \cong \Delta n(\omega_1 + n_+X_{11} + \tfrac{1}{2}m_+X_{12}) + \Delta m(\omega_2 + m_+X_{22} + \tfrac{1}{2}n_+X_{12}), \tag{10}$$
$$n_+ = n + n', \quad \Delta n = n - n',$$
$$m_+ = m + m', \quad \Delta m = m - m',$$

and Y_{222} has been neglected.

Equation (9) (equivalent to the expression for a Lyot filter) clearly shows that multiple interferences between energy levels determine the temporal evolution of $|C(t)|^2$.

The discrete sum of the energy gaps can be replaced by a continuous sum where the distribution of the energy gaps can be introduced. The theory of random matrices[20,8,12] then allows us to calculate the evolution of the ensemble average of $|C(t)|^2$ and to extract the statistical properties. In the first instance, we will not proceed with the study of this ensemble average since this procedure masks important effects and the molecular Hamiltonian is far from being a random matrix. In order to gain a good understanding of what we observe in the FT spectrum, we will progress from a single oscillator to two oscillators and from the harmonic case to the anharmonic case.

Figure 1 represents $|C(t)|^2$ for the bending oscillation of CS_2. We clearly see that the effect of the anharmonicities is to widen the peaks of the harmonic oscillator in a direction which depends on the sign of the anharmonicity. The edges of a packet correspond to the times pT_- and pT_+, where p is the number of the peak observed in the FT and

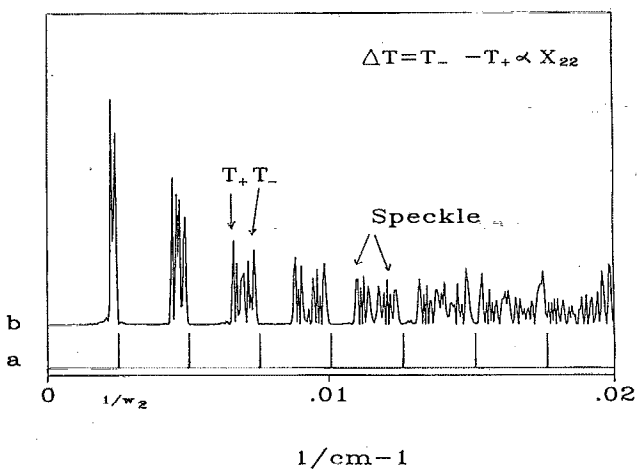

FIG. 1. Square of the FT $|C(t)|^2$ of the spectrum of the bending mode of CS_2 from 0 to 12 000 cm^{-1}. (a) Harmonic oscillator ($E = \omega_2 m$); (b) anharmonic oscillator ($E = \omega_2 m + X_{22}m^2 + Y_{222}m^3$). No unfolding has been performed on the spectrum before taking the FT in order that the characteristic times of the molecule should not be lost. We note the widening of the peaks due to the anharmonicities. The width of the peak p is $\Delta T \cong p(h/\omega_2^2)m_{+\max}X_{22}$. This width measures the degree of anharmonicity which is large in CS_2.

$$T_- = \frac{h}{\omega_2},$$

$$T_+ \cong \frac{h}{\omega_2 + m_{+\max} X_{22}}. \tag{11}$$

T_- corresponds to the low-energy part of the spectrum ($m_+ \sim 0$) and, therefore, to the harmonic case; T_+ corresponds to the high-energy part of the spectrum ($m_+ = m_{+\max}$). The width ΔT of the packet is a direct measure of the anharmonicities

$$\Delta T \approx p \frac{h}{\omega_2^2} m_{+\max} X_{22}. \tag{12}$$

Figure 2 represents the case of two harmonic oscillators (Fig. 2(a): $\omega_1, \omega_2 \neq 0$) and two anharmonic oscillators (Fig. 2(b): $\omega_1, \omega_2, X_{11}, X_{22}\ X_{12} \neq 0$).

We clearly observe a stroboscopic peak which corresponds in the harmonic and anharmonic cases (the coupled anharmonic case being the most complex) to

$$\frac{\Delta n}{\Delta m} = \frac{2\omega_2}{\omega_1} \cong \frac{6}{5} \quad \text{(harmonic case)}, \tag{13}$$

$$\frac{\Delta n}{\Delta m} \approx \frac{\omega_1 + n_+ X_{11}}{\omega_2 + m_+ X_{22}} \approx \frac{5}{4} \quad \text{(anharmonic case)}, \tag{14}$$

and to a stroboscopic time

$$T_s^{\mathrm{h}} = \frac{5}{\omega_1} \approx \frac{6}{2\omega_2} = 6\ \mathrm{T_0},$$

$$T_s^{\mathrm{an}} \approx \frac{4}{\omega_1} \approx \frac{5}{2\omega_2} = 5\ \mathrm{T_0}, \tag{15}$$

where T_0 is the shortest periodic orbit period [see Figs. 2(a), 2(b), and 2(c)]. The relative intensities between the stroboscopic peaks and the other peaks depends on how close to an integer are Δn and Δm. For exact integers the stroboscopic peaks are all equal to 1 and the others vanish.

Classically, this stroboscopic peak corresponds to the fact that a particular trajectory turns Δn times in the stretching direction and Δm times in the bending direction before returning to the same point. On the average, the effect of this stroboscopy is to make a "stroboscopic hole"[21] [see Fig. 3(a)] appear at the origin of the FT. This hole exists for a perfectly deterministic system and has nothing to do with the "correlation hole" which occurs in the context of random matrices for a chaotic system. It is important to note that when we take account of the anharmonicities and the couplings, the peaks and the stroboscopic hole are attenuated and contract towards the time origin [Figs. 2(a), 2(b), and 2(c)]. For CS_2 ($E < 12\,000\ \mathrm{cm}^{-1}$) the width of the stroboscopic hole is of the order of Td/10 [see Fig. 3(a)], where Td is the time corresponding to the mean density of states. The width of the correlation hole is Td. Therefore, in the case of a largely anharmonic molecule like CS_2, this stroboscopic hole is not a great problem. It is important to note that the stroboscopic hole does not correspond to the general observation of Berry that a spectrum is rigid for energy intervals beyond the inverse of the shortest closed orbit (that is to say, in the time domain, this effect is observable at time

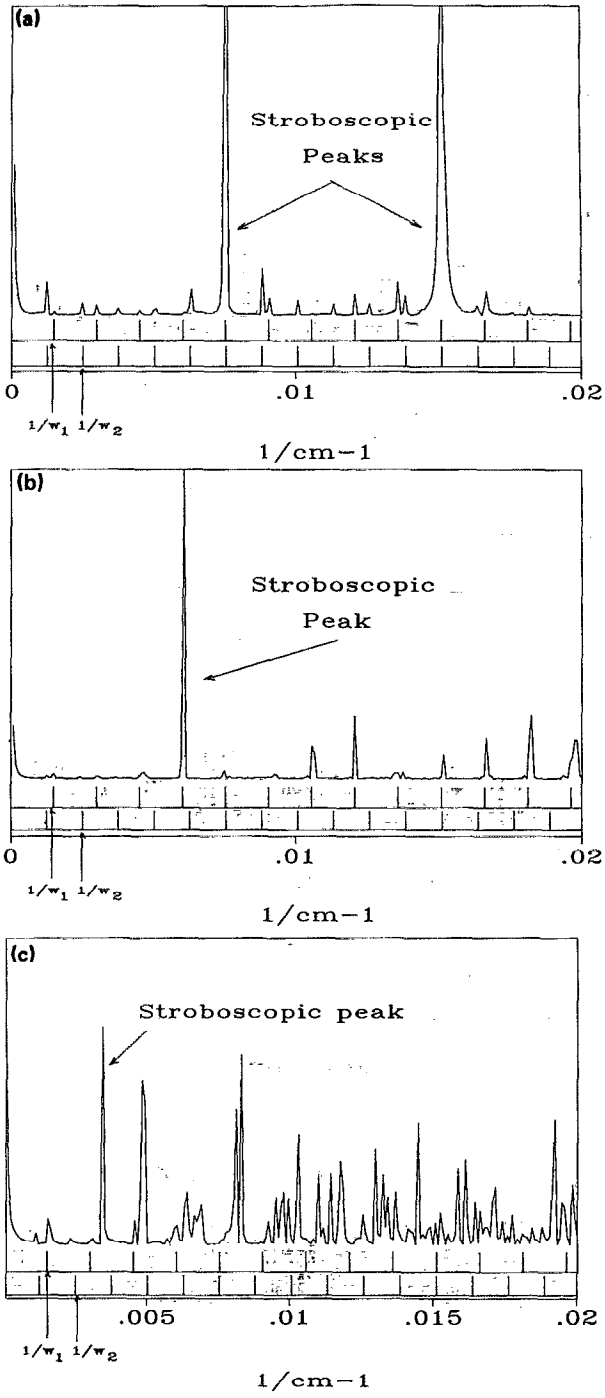

FIG. 2. Square of the Fourier transform $|C(t)|^2$ of the spectrum generated by the bending and symmetric stretching oscillations of CS_2 from 0 to 12 000 cm^{-1}. The regular peaks correspond to two harmonic oscillators which serve as markers. (a) The case of two harmonic oscillators ($E = n\omega_1 + m\omega_2$). For reasons of symmetry only an even number of quanta appear in the bending mode. Moreover, for this mode the observed frequency is $2\omega_2$. We can see a definite stroboscopic peak at times $T_S \sim 5/\omega_1 \sim 6/2\omega_2$ and recurrences at times $2T_S$. This peak corresponds to a constructive interference effect (see text). (b) The case of two anharmonic oscillators ($E = n\omega_1 + m\omega_2 + n^2X_{11} + m^2X_{22} + nmX_{12}$). The stroboscopic peak decreases in intensity and moves towards the time origin. (c) The case of two anharmonic oscillators in Fermi resonance. The spectrum results from the diagonalization of the Hamiltonian described earlier. The stroboscopic peak is attenuated and moves to shorter times. The stroboscopic time T_S is small compared with the time corresponding to the mean density of states Td ($T_S \sim$ Td/10). This results from the fact that CS_2 is very anharmonic.

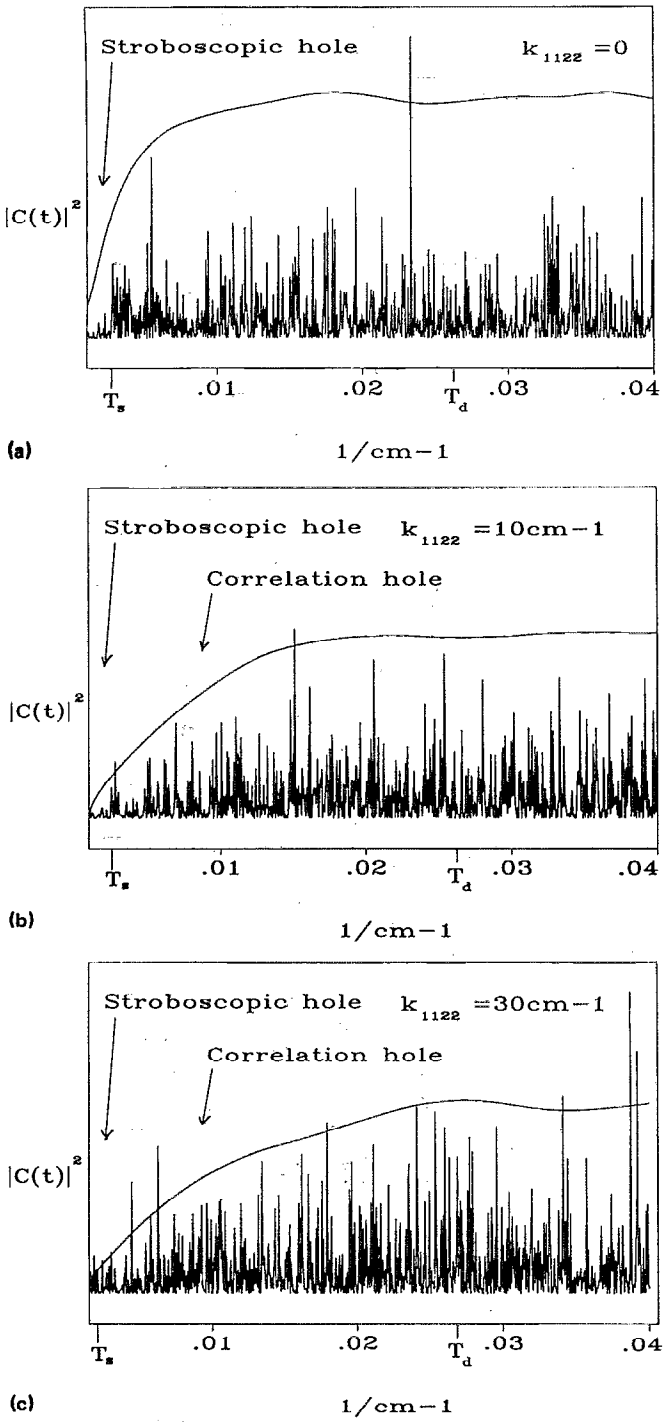

FIG. 3. Square of the Fourier transform $|C(t)|^2$ of the spectrum of two anharmonic oscillators in Fermi resonance and coupled by the nonintegrable coupling H_C described by the parameter k_{1122} and which couples nearest-neighbor polyads. (a) Noncoupled case: $k_{1122}=0$. We note the stroboscopic hole whose width is about Td/10. (b) and (c) Coupled case: $k_{1122}=10$ cm^{-1} and $k_{1122}=30$ cm^{-1}. A correlation hole is superimposed on the stroboscopic hole. This hole enlarges as the coupling increases. Its maximum width is Td.

shorter than the time T_0 of the shortest periodic orbit). The effect of the stoboscopic hole begins after T_0 and stops at a longer time depending on the anharmonicities [it is about $10T_0$ for the example in Fig. 3(a)]. The existence of this stroboscopic hole prevents a general study of the onset of the transition to chaos by analysis of $|C(t)|^2$. In contrast, we will see later that it is possible, in the case of CS_2, to carry out a detailed study of the phase space structure which is much more sensitive to the appearance of the first nucleation zones of chaos.

Figure 3 shows the nonaveraged $|C(t)|^2$ and $|C(t)|^2$ averaged by means of the dichotomic convoluted windows (DCW) procedure described in Ref. 12 for both H_0+H_F and $H=H_0+H_F+H_C$ (which includes coupling between adjacent polyads). Figure 3(a) corresponds to the noncoupled case ($k_{1122}=0$) and clearly shows the stroboscopic hole whose width is about Td/10. As k_{1122} increases, the correlation hole widens and deepens [Figs. 3(b) and 3(c)] in agreement with theory,[8,12,20] which predicts that the ensemble average of the slowly varying component of $\langle|C(t)|^2\rangle$ is given by

$$\langle|C(t)|^2\rangle = N[1-b_2(t)]\otimes\frac{\sin^2\Delta E_{\max}t}{(\Delta E_{\max}t)^2}, \qquad (16)$$

where $\otimes$ represents a convolution product, N is the number of levels in the spectrum, $\Delta E_{\max}$ is the energy range of the spectrum, and $b_2(t)$ is the Fourier transform of the Mehta cluster function which describes the spectral correlations. If H_C were integrable, then k_{1122} would play the same role as the anharmonicities which tend, as we have seen earlier, to reduce the width of the stroboscopic hole. The fact that the hole widens with increasing k_{1122} and reaches a final value of Td, shows that H_C renders the Hamiltonian of CS_2 nonintegrable and leads to a chaotic situation. H_C is one of the lowest-order terms that efficiently couples the nearest-neighbor polyads of CS_2. This fact will be confirmed below by the phase-space analysis.

IV. DYNAMICS OF THE CLASSICAL OBJECT: STRUCTURE OF THE PHASE SPACE OF CS_2

We now pose the following question: How do we extract the molecular dynamics from the spectroscopy of the molecule? The patterns contained in the spectrum have a shape which is often very relevant to the topology of the phase space of the corresponding classical object. Furthermore, as we have just seen, in general, statistical methods do not allow us to study the onset of the transition to chaos. In contrast, the study of phase space is much more sensitive. The approach which would consist of working in the space of normal configurations ($\{p_i,q_i\}$) is meaningless for CS_2, partly because of the strong Fermi couplings which mix the normal modes and partly because a polynomial expansion of the potential in p_i,q_i at a given order, introduces numerous additional parameters (not fitted) and couplings which have no physical meaning within the framework of perturbation theory. Instead we use a method developed by several authors and, in particular, an extension of Kellman's theory[19] which is well adapted to the case of CS_2 since, firstly, at the energies that concern us in this paper, the problem reduces to a system of two dimensions and, secondly, CS_2 is subject to strong Fermi resonances. Our aim is to make an unequivocal correspondence between the effective Hamiltonian fitted to

the experimental data and the semiclassical Hamiltonian, and to define the best basis which includes the integrable resonances. The method is based on the Heisenberg correspondence principle and on the definition of a vibrational angular momentum operating in the Lie group SU(2).[22–25]

We will briefly review the definitions that we adapt to the case of CS_2 while retaining the spectroscopists notation. The Hamiltonian described earlier can be rewritten in the second quantization as

$$\begin{aligned} H_0 &= \omega_1'(v_1+\tfrac{1}{2}) \\ &\quad + \omega_2'(v_2+1) + X_{11}(v_1+\tfrac{1}{2})^2 + X_{22}(v_2+1)^2 \\ &\quad + X_{12}(v_1+\tfrac{1}{2})(v_2+1) + Y_{222}(v_2+1)^3, \qquad (17) \\ H_F &= +(1/2\sqrt{2})k_{122}(a_1^\dagger a_2 a_2 + a_1 a_2^\dagger a_2^\dagger), \\ H_C &= k_{1122}(a_1^\dagger a_1^\dagger a_2 a_2 + a_1 a_1 a_2^\dagger a_2^\dagger), \end{aligned}$$

where $a_i^\dagger$ and a_i are the vibrational creation and annihilation operators of the stretching and bending modes. Several terms (13) can, like H_c, couple adjacent polyads. They come from cubic, quintic, and sixtic combinations of the a_i. It is interesting to note that H_F and the cubic term

$$(1/2\sqrt{2})k'_{122}(a_1 a_2 a_2^\dagger + a_1^\dagger a_2^\dagger a_2),$$

which couple adjacent polyads with the selection rules $\{\Delta v_1 = \pm 1,\ \Delta v_2 = 0\}$, come from the same classical cubic term $k_{122}Q_1Q_2Q_2$ of the normal-mode representation. But it is important to separate them because below 12 000 cm^{-1}, H_F is a strong coupling which leave the Hamiltonian separable, while k'_{122} which is experimentally nonobserved (excepted, may be, for accidental levels anticrossings), render the CS_2 Hamiltonian nonintegrable.

The Heisenberg correspondence principle allows us to make the correspondence between this effective (quantum) Hamiltonian and the semiclassical Hamiltonian. The creation and annihilation operators can be substituted using two different forms,

$$\begin{aligned} a_i^\dagger &= \frac{1}{\sqrt{2}}(q_i + ip_i), \\ a_i &= \frac{1}{\sqrt{2}}(q_i - ip_i) \quad (i=1,2), \qquad (18) \\ a_i^\dagger &= \left(n_i + \frac{d_i}{2}\right)^{1/2} e^{+i\phi_i}, \\ a_i &= \left(n_i + \frac{d_i}{2}\right)^{1/2} e^{-i\phi_i}, \qquad (19) \end{aligned}$$

where d_i is the degeneracy of the vibron, $[n_i + (d_i/2)]^{1/2}$ is the action variable, and ϕ_i is the conjugate angle variable.

The form given by Eqs. (18) allows us to express each term of H in the system of normal coordinates. Like Kellman,[19] we prefer the form given in Eqs. (19) which allows an elegant treatment of the 1:2 Fermi resonance. The vibrational angular momentum of SU(2) is defined by

$$\begin{aligned} I &= \tfrac{1}{2}(a_1^\dagger a_1 + a_2^\dagger a_2/2) = \tfrac{1}{2}(n_1 + n_2/2) = \frac{N}{2}, \\ I_z &= \frac{1}{2}(a_1^\dagger a_1 - a_2^\dagger a_2/2) = \tfrac{1}{2}(n_1 - n_2/2) = \frac{M}{2}, \\ I_x &= \frac{1}{2}(a_1^\dagger a_2 a_2 + a_1 a_2^\dagger a_2^\dagger)/(a_2^\dagger a_2)^{1/2}, \\ I_y &= \frac{-i}{2}(a_1^\dagger a_2 a_2 - a_1 a_2^\dagger a_2^\dagger)/(a_2^\dagger a_2)^{1/2}. \end{aligned}$$

Note that $2I$ is the number of the polyad and $2I_z$ is the order number in the polyad. I_x represents the Fermi coupling term H_F. The components of the angular momentum can be represented semiclassically using the correspondence given in Eqs. (19) (Table II). The conjugate angle variable $\theta = \phi_1 + 2\phi_2$ et $\psi = \phi_1 - 2\phi_2$ correspond to the action variables I and I_z. The different terms of the effective Hamiltonian can then be expressed as a function of these new variables. Table III gives the result (even for the higher-order Fermi couplings introduced and described by the λ_i parameters).

The enormous advantage of this representation is, on the one hand, to make a simple, unequivocal correspondence between the experimental spectrum and the semiclassical Hamiltonian, and, on the other hand, to define a constant of motion which includes the Fermi resonances. In effect, we see that, if we limit ourselves to H_0, I and I_z are the constants of motion since

$$\begin{aligned} \frac{dI}{dt} &= \frac{\partial H_0}{\partial \theta} = 0, \\ \frac{dI_z}{dt} &= \frac{\partial H_0}{\partial \psi} = 0, \qquad (20) \end{aligned}$$

so H_0 is integrable and I and I_z are good quantum numbers.

In contrast, for $H_0 + H_F$, we have only

$$\frac{dI}{dt} = \frac{\partial(H_0 + H_F)}{\partial \theta} = 0(21). \qquad (21)$$

However, for a system of two degrees of freedom, $H_0 + H_F$

TABLE II. Quantum and semiclassical definition of the vibrational angular momentum **I**.

	Quantum	Semiclassical
I	$\tfrac{1}{2}(a_1^\dagger a_1 + a_2^\dagger a_2/2) = N/2$	$\tfrac{1}{2}(n_1 + n_2/2 + 1) = (N+1)/2$
I_z	$\tfrac{1}{2}(a_1^\dagger a_1 - a_2^\dagger a_2/2) = M/2$	$\tfrac{1}{2}(n_1 - n_2/2) = M/2$
I_x	$\tfrac{1}{2}(a_1^\dagger a_2 a_2 + a_1 a_2^\dagger a_2^\dagger)/(a_2 + a_2)^{1/2}$	$(I^2 - I_z^2)^{1/2}\cos\psi$
I_y	$-i/2\,(a_1^\dagger a_2 a_2 - a_1 a_2^\dagger a_2^\dagger)/(a_2^\dagger a_2)^{1/2}$	$(I^2 - I_z^2)^{1/2}\sin\psi$

TABLE III. Quantum and semiclassical correspondence of the different terms of the vibrational Hamiltonian of CS_2 using the vibrational angular momentum coordinates.

	Quantic	Semiclassic
H_0	$\omega_0(2I+1)+PI_z+\frac{1}{2}Q(2I+1)I_z+\alpha_1[I(I+1)+\frac{1}{4}]+\alpha_2 I_z^2$ $+y_{222}(2I+1-2I_z)^3$	$\omega_0 2I+PI_z+QII_z+\alpha_1 I^2+\alpha_2 I_z^2+y_{222}[2(I-I_z)]^3$
H_F	$+k_{122}I_x\sqrt{I-I_z}$	$+k_{122}\sqrt{I+I_z}(I-I_z)\cos\psi$
H_C	$\sqrt{2}k_{1122}(a_1^\dagger I_+ + I_- a_1)(I-I_z)^{1/2}$	$4k_{1122}(I^2-I_z^2)\cos\left(\frac{3\psi+\theta}{2}\right)$
λ_1	$\sqrt{2}\lambda_1(I+I_z)I_x\sqrt{I-I_z}$	$2\lambda_1(I+I_z)^{3/2}(I-I_z)\cos\psi$
λ_2	$2\sqrt{2}\lambda_2(I-I_z)I_x\sqrt{I-I_z}$	$4\lambda_2(I+I_z)^{1/2}(I-I_z)^2\cos\psi$
k'_{122}	$2k'_{122}(I-I_z)(a_1+a_1^\dagger)$	$4k'_{122}(I-I_z)\sqrt{I+I_z}\cos\left(\frac{\psi+\theta}{2}\right)$

remain integrable and I remains a good quantum number. The second action variable is

$$S=\oint I_z d\psi. \tag{22}$$

S does not have a simple analytical expression due to the strong Fermi resonance.

To make the Hamiltonian nonintegrable, it is necessary to introduce a coupling of the type H_C between polyads. In effect, because H_C is a function of θ and ψ, we have, for $H=H_0+H_F+H_C$,

$$\frac{dI}{dt}=\frac{\partial H}{\partial\theta}\neq 0, \tag{23}$$

$$\frac{dI_z}{dt}=\frac{\partial H}{\partial\psi}\neq 0. \tag{24}$$

We will now discuss the structure of the phase space for the case where the Hamiltonian is most integrable, that is, for H_0+H_F. The profile of the phase space can be obtained either by finding a numerical solution of Hamilton's equations,

$$\frac{dI_z}{dt}=\frac{\partial(H_0+H_F)}{\partial\psi},$$
$$\frac{d\varphi}{dt}=-\frac{(\partial H_0+H_F)}{\partial I_z}, \tag{25}$$

or by tracing the contour plot of $H(I_z,\psi,I_0)$ for a given polyad ($2I_0=\text{const}$). The first method has the advantage that it allows us to measure the orbital periods which allows a link to be made with analysis of the spectra by FT. It has the further advantage that it allows the introduction of couplings such as H_C. The topology of the phase space can be studied on the polyad phase sphere (PPS) of radius I_0 and coordinates I_x, I_y, I_z, or in the space E, I_z, ψ. Figures 4 and 5 give the two representations for the polyad $N=18$.

A correspondence can be established between the periodic orbits and the eigenstates of $H=H_0+H_F$. Each traced orbit corresponds to an energy taken to be equal to the experimentally measured energy of a level of the eighteenth polyad. In Fig. 4 the trajectories on the PPS correspond to the precession of the vibrational angular momentum **I** which varies gradually from the direction I_x to the direction I_y.

This is a typical motion for a strong Fermi resonance. For the non-Fermi-resonance Hamiltonian H_0 the precession of **I** stays in the I_z direction as I_z is a good quantum number of H_0. The trajectories of Fig. 6(b) are level contours of $H=H_0+H_F$ for each experimental level of the polyad. The fixed points labeled + and − on Fig. 6(b), correspond to a maximum and minimum of the energy. These fixed points give the stroboscopic effect noted in the FT analysis of the quantum spectra. They correspond to the fact that, in the space of normal coordinates, the corresponding trajectory turns Δn times in the stretching direction while turning Δm times in the bending direction. We notice two types of trajectory: those (type I) which are localized close to the fixed

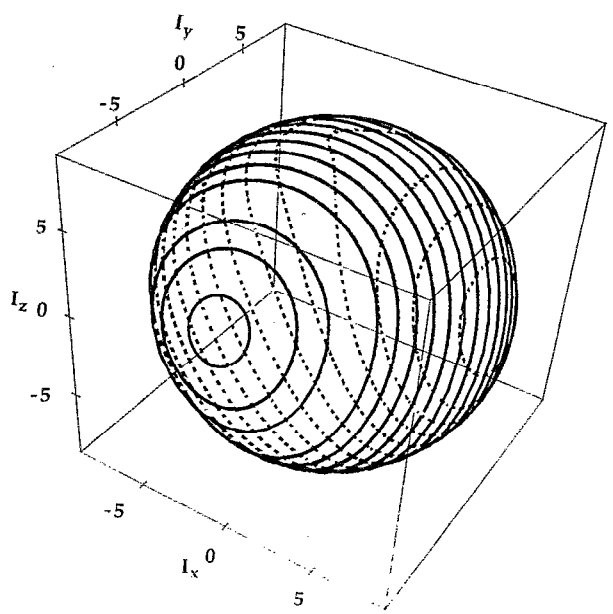

FIG. 4. Representation of trajectories for each quantum level of polyad $N=2I_0=n_1+n_2/2=18$ on the polyad sphere defined in the space I_x, I_y, I_z, the radius being equal to the constant of motion I_0. The I_z direction represents the order number of the Hamiltonian H_0 (see text) in the polyad, and the I_x direction represents the coupling term of the 1:2 Fermi resonance of CS_2.

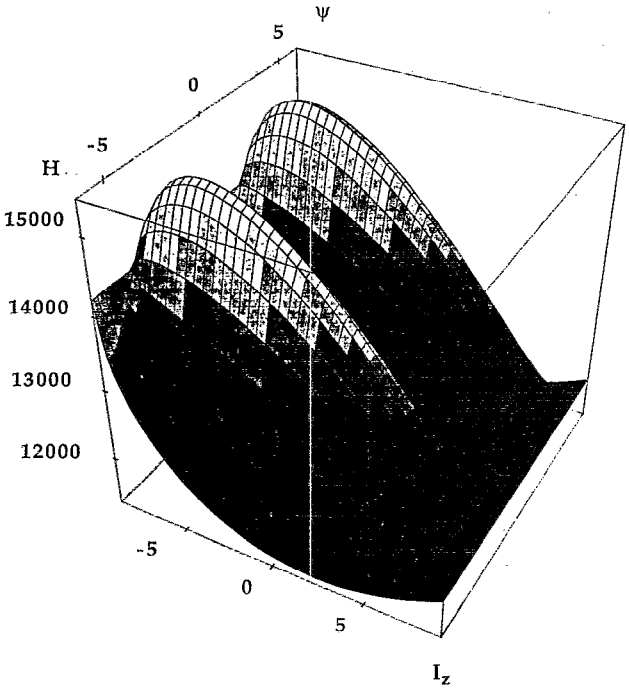

FIG. 5. Energy surface of polyad 18 as a function of I_z and its conjugate ψ for the Hamiltonian $H = H_0 + H_F$ (see text). The maximum corresponds to those states which are mostly bending in character ($I_z \cong -I_0$) whilst the minimum corresponds to stretching states ($I_z \cong +I_0$).

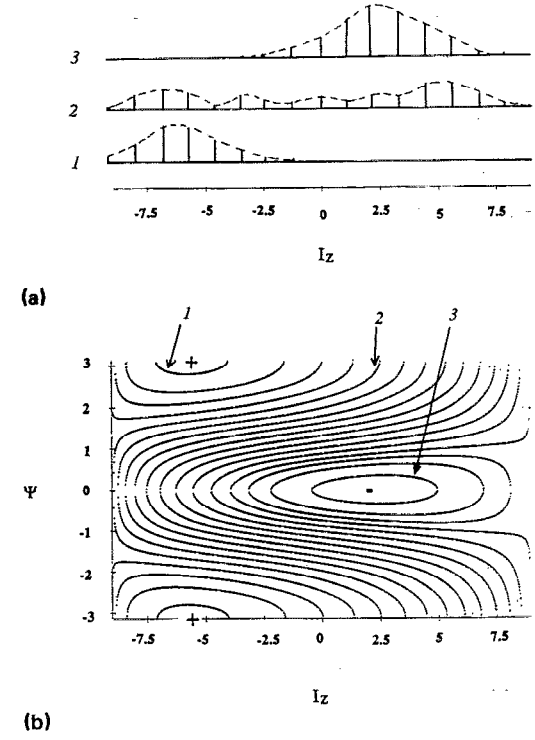

FIG. 6. (a) Contour plot corresponding to the energy of the polyad as a function of the conjugate variables I_z and ψ. Each level curve or trajectory represents the energy of a quantum level of the $N = 18$ polyad. The fixed points correspond to the stroboscopic effect observed in the FT of the spectra. We note two types of trajectory: those which go around the fixed points (type I) and those which avoid the fixed points and wind around a cylinder (type II). The type I trajectories are more localized than type II. We note that there are two separatrices situated between the two types of trajectory. (b) Representation in the H_0 basis of three wave packets corresponding to three eigenstates of $H_0 + H_F$ in polyad 18. The width along I_z of these wave packets corresponds exactly to the localization width of the periodic orbits.

points and which wind around them and those (type II) which avoid the fixed points and wind between the fixed points on a cylinder. Figure 6(a) shows the decomposition of the eigenstates of $H_0 + H_F$ on the H_0 basis for which $I_z = I_0$ corresponds to a pure stretching state and $I_z = -I_0$ corresponds to a pure bending state. We have shown three eigenstates of $H_0 + H_F$ for which the energy corresponds exactly to the trajectories (labeled 1, 2, 3) in Fig. 6(b). These states can be written in the H_0 basis as

$$|e\rangle = \sum_{I_z=-I_0}^{+I_0} C_{I_z} |I_z\rangle. \tag{26}$$

At this point we can make a precise analogy between the position of the trajectories in classical phase space and the width of the quantum wave packets. Figure 6 shows that the width ΔI_z of the three wave packets corresponding to the three eigenstates under consideration is approximately equal to the extent of the trajectory along I_z. The most localized states correspond to type-I trajectories and the most delocalized states to type-II trajectories. This example shows that the description of the vibrational Hamiltonian of CS_2 in the basis described by the vibrational angular momentum **I** is well adapted to show the classical quantum correspondence because it includes the nonlinearities due to the Fermi resonances. It is therefore interesting to study the topology of phase space when there exists a nonintegrable nonlinearity of the type introduced by H_C which couples neighboring polyads. Figure 7 represents the evolution of the trajectories of polyad 18 when the parameter k_{1122} is taken to be equal to 1 cm^{-1}. The result is in agreement with the general predictions of the theory of chaos: the trajectories which destabilize first are situated near to the separatrix between type-I and type-II trajectories and which correspond to the most delocalized states. The nucleation of the first chaotic

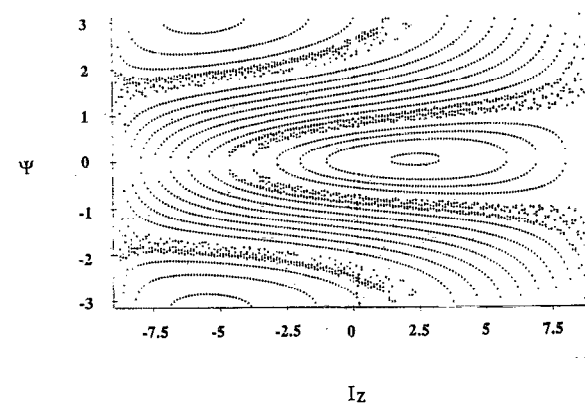

FIG. 7. Trajectories for polyad 18 in the presence of a weak, nonintegrable coupling H_C corresponding to $k_{1122} = 1$ cm^{-1}. Note the destabilization of the most delocalized periodic orbits near to the separatrices between the two types (I and II) of motion.

zones is clearly visible in Fig. 7. As one increases the value of k_{1122}, the region of phase space which is taken over by chaotic motion increases around these nucleation zones. The most stable trajectories are located near the fixed points. Hence, even for small values of k_{1122} the onset of chaos is clearly visible in the phase-space analysis.

In contrast, the Fourier transform analysis of the quantum spectra for $k_{1122} = 1\ \mathrm{cm}^{-1}$ has not allowed us to observe the spectral correlations since they do not emerge above the statistical noise and also because of the existence of the stroboscopic hole. We have diagonalized the matrix corresponding to $H_0 + H_F + H_C$ for the values of the parameters given in Table I and for $k_{1122} = 1\ \mathrm{cm}^{-1}$; we then have attempted to observe, the correlation hole in the spectrum thus obtained, and have also studied the statistical functions such as the nearest-neighbor distribution. In all cases the result is statistically indistinguishable from that obtained from the spectrum generated by the integrable Hamiltonian $H_0 + H_F$. Thus, we see that the intrinsic noise in statistical methods is a significant limitation in the study of the transition to chaos. Furthermore, the physical significance of these methods is not always obvious in molecular physics. It seems to us that phase-space analysis is the most sensitive and often the most instructive. This method, however, requires us to extract from the experimental spectra the "most integrable basis" in order to obtain a simple phase-space topology with, in particular, well-marked separatrices which do not constantly change as various parameters change. For CS_2, the vibrational angular basis described by **I** is better adapted than the normal basis because I is a good quantum number of $H_0 + H_F$.

V. CONCLUSION

We have shown in this paper that, using high-quality vibrational spectra of CS_2, it was possible to carry out an experimental and theoretical investigation of the transition to vibrational chaos. A description in terms of normal modes is not suitable for CS_2 due to the strong Fermi resonances. The enormous advantage of the vibrational angular momentum basis is that it includes the 1:2 Fermi resonance in the integrable zero-order Hamiltonian, and that it provides a simple phase space, the topology of which strongly resembles that of already well-studied theoretical models. The nonlinear and nonintegrable terms are described equally simply both classically and quantum mechanically in this basis. This allows us to set up a quantum classical analogy. We have shown in this paper that statistical methods do not allow the observation of the onset of the transition to chaos on account of the intrinsic noise of these methods.

A possible scenario for CS_2 is the progressive appearance of nonlinearities such as the one described by the parameter k_{1122}. This nonlinearity is simply a 2:2 resonance. In fact, even at low energy the corresponding nonintegrable coupling can be observed in the case of accidental energy level crossing.[18] In a system of two degrees of freedom, at least two resonances of different order are necessary to render the Hamiltonian nonintegrable. We check different forms for the coupling H_c corresponding to different orders in the product of the operators a_i. Every additional n:m type resonance (except the 1:2) leads to the same conclusion: the statistical properties and phase-space modifications are similar.

Our aim is to study the entire potential of the ground state of CS_2 from the bottom of the well to the first dissociation limit. We have measured the vibrational spectrum at high resolution up to 19 500 cm^{-1}. The analysis of the results between 12 000 and 19 500 cm^{-1} is in progress.

ACKNOWLEDGMENTS

This work was supported by Contract No. 900.3/1308V5655 with the French Conseil Régional de la Région Rhône-Alpes and Contract No. SCI-0034-CCD with the European Economic Community.

[1] O. Bohigas and M. J. Giannoni, *Chaotic Motion and Random Matrix Theories*, Vol. 209 of Lecture Notes in Physics (Springer Verlag, Berlin, 1984); *Chaos and Quantum Physics*, edited by A. Voros and M. J. Giannoni (North Holland, Amsterdam, 1990).
[2] E. Abramson, R. W. Field, D. Imre, K. K. Innes, and J. L. Kinsey, J. Chem. Phys. **80**, 2298 (1984).
[3] E. P. Wigner, Phys. Rev. **40**, 749 (1932).
[4] J. P. Pique, Y. Chen, R. W. Field, and J. L. Kinsey, Phys. Rev. Lett. **58**, 475 (1987).
[5] J. P. Pique, M. Lombardi, Y. Chen, R. W. Field, and J. L. Kinsey, Ber. Bunsenges. Phys. Chem. **92**, 422 (1988).
[6] E. Haller, H. Köppel, and L. S. Cederbaum, Phys. Rev. Lett. **52**, 1665 (1984).
[7] R. Jost and A. Delon (private communication).
[8] L. Leviandier, M. Lombardi, R. Jost, and J. P. Pique, Phys. Rev. Lett. **56**, 2449 (1986).
[9] M. Broyer, G. Delacretaz, C. Q. Ni, R. L. Whetten, J. P. Wolf, and L. Wöste, J. Chem. Phys. **90**, 4620 (1989).
[10] J. A. Bentley, J. P. Brunet, R. E. Wyatt, R. A. Friesner, and C. Leforestier, Chem. Phys. Lett. **161**, 393 (1989).
[11] K. Yamanouchi, S. Takeuchi, and S. Tsuchiya, J. Chem. Phys. **92**, 4044 (1990).
[12] J. P. Pique J. Opt. Soc. Am. B **7**, 1816 (1990).
[13] J. M. Gomez-Llorente, S. C. Farantos, O. Hahn, and H. S. Taylor, J. Opt. Soc. Am. B **7**, 1851 (1990).
[14] J. Main, G. Wiebush, and K. H. Welge, Comm. At. Mol. Phys. **25**, 233 (1991).
[15] B. Eckhardt, Comm. At. Mol. Phys. **25**, 273 (1991).
[16] S. Kato, J. Chem. Phys. **82**, 3020 (1985).
[17] B. Kleman, Can. J. Phys. **41**, 2034 (1963).
[18] J. P. Pique, J. Manners, M. Joyeux, and G. Sitja (unpublished).
[19] Z. Li, L. Xiao, and M. E. Kellman, J. Chem. Phys. **92**, 2251 (1990).
[20] J. M. Delory and C. Tric, Chem. Phys. **3**, 54 (1974).
[21] M. Lombardi, J. P. Pique, P. Labastie, M. Broyer, and T. Seligman, Comments At. Mol. Phys. **25**, 345 (1991).
[22] C. C. Martens and G. S. Ezra, J. Chem. Phys. **86**, 279 (1987).
[23] M. E. Kellman and E. D. Lynch, J. Chem. Phys. **85**, 7216 (1986).
[24] D. Farrelly, J. Chem. Phys. **85**, 2119 (1986).
[25] M. E. Kellman and E. D. Lynch, J. Chem. Phys. **88**, 2205 (1988).
[26] I. C. Perceval and N. Pomphrey, Mol. Phys. **35**, 649 (1978).